Recovering Displacements and Transients from Strong Motion Records Using the Wavelet Transform

A. A. Chanerley
School of Architecture, Computing & Engineering, University of East London, UK

N. A. Alexander
Department of Civil Engineering, University of Bristol, UK

SUMMARY:
Recovering the displacement time history from the acceleration record has been the subject of much research over several decades. The problem is caused by drifts in the baseline of the acceleration time history, which after double-time integration lead to dc shifts in the velocity and linear and/or quadratic trends in the displacement time history. This paper demonstrates a method yields results which other methods have not been able to produce. The core of the method is the application of the bi-orthogonal wavelet transform with which to filter and decimate the time history. This produces a low-frequency time series (the 'fling') as well as the higher frequencies. The acceleration offsets and dc shifts are automatically corrected by the algorithm. It is inferred that the recovered transients may be due to ground tilts/rotations. The results are based on the 1999 Chi-Chi event using stations TCU052 and TCU129.

Keywords: correction, CUSP, double-integration, wavelet transform, fling,

1. INTRODUCTION

Current and previous methods for obtaining displacement time histories from recorder accelerations are sophisticated and varied. (Grazier, 1979) applied a baseline correction method by fitting a straight line to a segment of the velocity. (Iwan *et al.* 1985) removed pulses and steps from the acceleration time history by locating time points which exceeded a particular level of acceleration. (Boore 2001), and (Akkar & Boore, 2009) generalized this by adding further time points, which were not dependant on acceleration thresholds, the accumulated effects of these baseline changes represented by average offsets in the baseline. (Wu, 2007) also used the method due to (Iwan *et al.* 1985) on the Chi-Chi event and defined three time points, using a flatness coefficient to define one of the time points. (Wang, *et al.* 2003) designed and removed pulses and steps fitted with amplitudes which gave the same areas as the slope of the displacement to achieve stable double integration. (Chen and Loh, 2007) used a procedural wavelet transform method, but do not recover the low-frequency 'fling', the key low-frequency time series which gives the low-frequency velocity pulse and residual ground displacement.

A novel wavelet transform method, which uses an algorithmic approach due to (Chanerley and Alexander, 2010) is presented in this paper to recover the displacement and the baseline error. The algorithm operates on recorded seismic data, recovers a low-frequency pulse, which often has an almost sinusoidal profile for the stronger events, and automatically corrects the pulse for any baseline errors and integrates to obtain the velocity pulse and the residual displacement. Essentially there is some similarity with the research work cited above, with the difference that the wavelet transform method due to (Chanerley and Alexander, 2010) actually locates the profile of the baseline error and its location in time, rather than use sophisticated procedures to estimate both the baseline error and its location in time.

Theoretical, low-frequency model 'flings' are basically sinusoids or co-sinusoids and similar low-frequency fling profiles are obtainable using discrete, wavelet filters. The wavelet filters can recover the uncorrected, low-frequency, acceleration-fling time history. Then baseline correction is applied, simply by zeroing the acceleration from the location of the time point, followed by double-time integrate to displacement as shown in (Chanerley, Alexander 2010) and in the results section of this paper. The transform also de-noises the higher frequencies, which do not require further processing for errors and integrate to displacement.

2. THE DISCRETE WAVELET TRANSFORM AND DE-NOISING

The discrete wavelet transform (DWT) are octave filters and these form the basis of the transform by filtering and down-sampling by 2 each time leading to narrower bandwidths. Figure 1 shows a typical DWT filtering and down-sampling arrangement in the time domain.

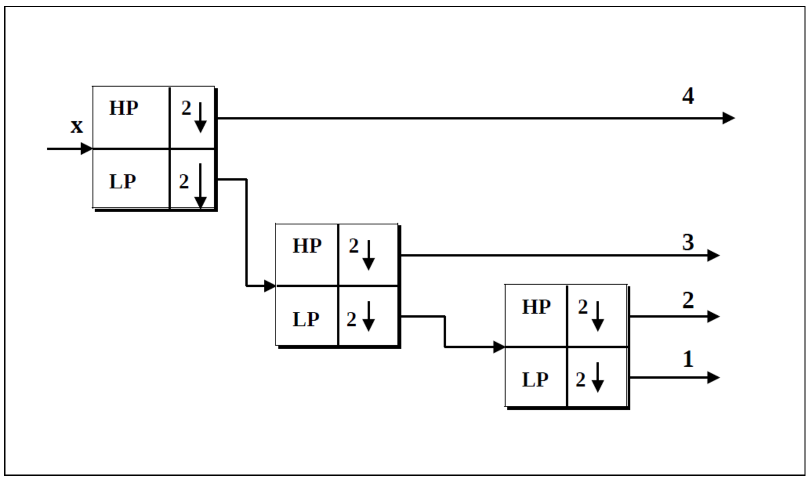

Figure 1. A 4-channel, analysis (decomposition) wavelet filter bank showing sub-bands

The filters are digital FIR filters for both the low-pass and high pass branches. These filters are also called non-recursive filters because the outputs depend only on the previous inputs and not on previous outputs. The behaviour of the filters is to operate on a vector of data by convoluting the data with the filter coefficients and to down- sample by 2, i.e. discard half the values. The inverse operation requires up-sampling by a factor of 2 followed by filtering and so the data is reconstructed in a translation invariant manner providing the reconstruction is performed using all the wavelet coefficients from all levels. (Mallat, 1989), (Daubachies, 1992), (Coifman, Wickerhauser, 1993) to name but a few of the key researchers in this area, who designed the filters and filter banks which then operate on the data as shown in the diagram of Figure (1). Wavelet filters are maximally flat filters and these applied with de-noising (Donoho and Johnstone 1994), (Coifman and Donoho 1995) yielded the results sought for all the components of the events as shown in (Chanerley, Alexander 2010) and (Chanerley, Alexander, Halldorsson 2009) and in this paper. However, because the DWT is not translation invariant i.e. it gives rise to aliasing between the sub-bands, therefore this would degrade any de-noising schemes which apply a threshold. Therefore instead we apply the stationary or translation invariant wavelet (SWT) transform (Donoho 1997), (Coifman, Donoho 1995). It is also referred to as the un-decimated transform, but essentially when using the SWT the data is filtered but not down-sampled, instead the filter coefficients are dyadically up- sampled therefore the length of the data in each branch is not half the previous length as with the DWT, but is equal to the length of the original data. The scheme is similar to that of Figure 1, but the down-samplers are removed and instead the filters are up- sampled versions of the previous filters by dyadically pushing zeros into the coefficients of the high-pass and low-pass filters, this has the same effect of reducing the band-width at each level, but without losing data due to down-sampling and shifting.

2.1 The De-Noising Scheme

The de-noising scheme with the SWT is essentially non-linear and yields a better root means square error than when used with the DWT. The point with regard to the de- noising scheme is that essentially it applies a threshold based on Donoho's (MAD/0.6745), (Median Absolute Deviation)/Scale Factor, where the scale factor is obtained by assuming a normal distribution of the noise and is also based on the standard deviation of the data multiplied by Dononho's 'root 2 log N'. The essential point is that the scheme is applied to both the low-frequency and high-frequency data obtained from the wavelet transform filters. This is to ensure that low-frequency noise and high frequency noise is removed from the wavelet transformed data.

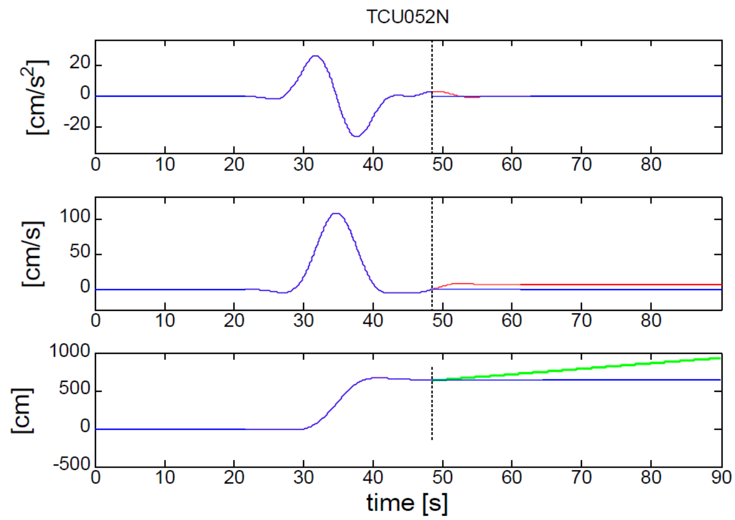

Figure 2. TCU052NS low-frequency sub-band, fling, which shows results before (red,green) and after (blue) baseline correction. The triangular area in the acceleration, the velocity and displacement offset at the dashed lines are the results of $g\varphi$ acceleration as described in (Boore, 2001) and (Grazier, 2005). Wavelet used is the *bior1.3*

3. RESULTS

3.1 Chi-Ch Station TCU052

TCU052, (Chanerley, Alexander, Halldorsson, 2009), shows similar low-frequency profiles to TCU068. The two stations are 10km apart for this event. Figure 2 shows the TCU052NS low frequency, almost sinusoidal fling profile obtained using the wavelet transform and then corrected for baseline error, which turns out to be acceleration transient. Only the low-frequency fling was corrected for baseline shift for TCU052, the higher frequencies did not require any baseline correction after processing by the wavelet transform. The time-histories of Figure 5 for the EW component show the resulting profiles after the low-frequency sub-bands were added to the higher frequencies.

The TCU052NS low-frequency, fling profile time-history of Figure 2, shows an acceleration tilt transient giving a peak acceleration of 3.015cm/s/s at 48.45 sec. Figure 2 shows the recovered tilt acceleration transient, which leads to a velocity offset and displacement trend after double-time integration of the transient. These are precisely the error offsets observed in the velocity and displacement time histories after double-time integrating the (almost) sinusoidal acceleration time history of Figure 1. It is inferred that acceleration transient of 3.015cm/s/s is in fact a $\boldsymbol{g\varphi}$ tilt transient. The area of the acceleration tilt profile is 7.21cm/s, which is the velocity offset. Similarly the area under the velocity step is 294.7cm, the maximum displacement offset as shown in Figure 2 and Figure 3. The corrected displacement is 641cm, which compares with those of other researchers, but GPS is

845cm. The point to note is that the area of the acceleration transient shown in Figure 3 and extracted from Figure 2, is exactly equal to the constant velocity offset shown after integrating the acceleration transient and observed in the velocity sub-band. Then after integrating the constant velocity offset, then the result matches exactly the linear trend in the displacement before correction.

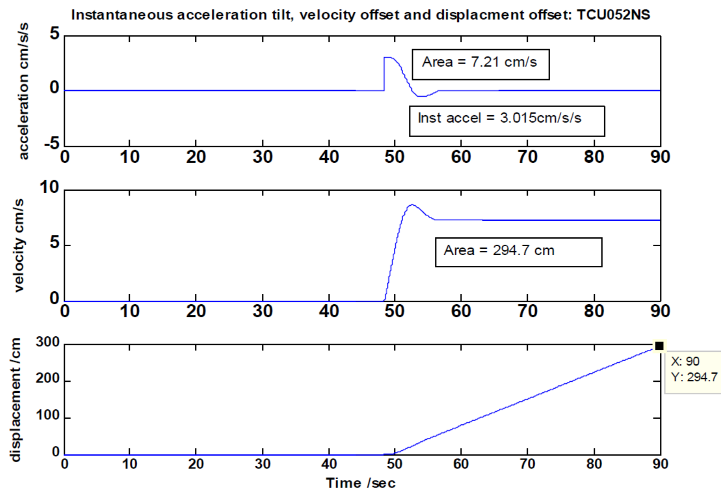

Figure 3. Velocity and displacement response of instrument (A900) to instantaneous acceleration tilt for the TCU052NS component

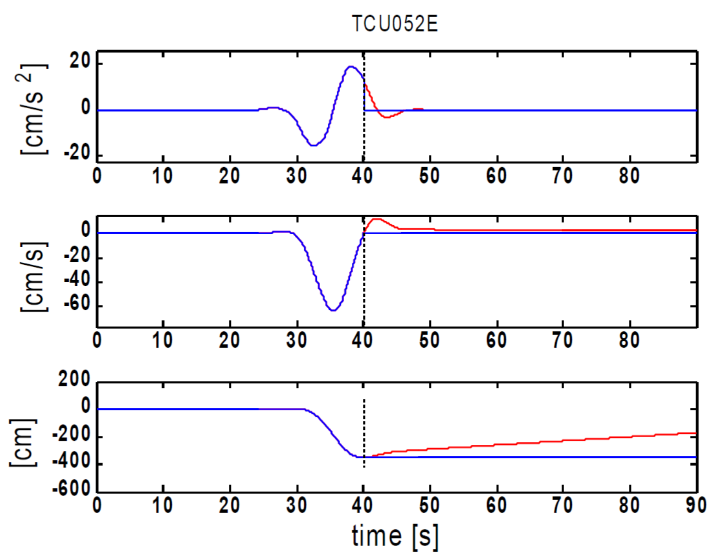

Figure 4. TCU052EW low-frequency sub-band, fling, which shows results before (red) and after baseline correction (blue). The triangular area in the acceleration, the velocity and displacement offset at the dashed lines are the results of gφ acceleration as described in (Boore, 2001) and (Grazier, 2005). The displacement is -352cm and the wavelet used is the bior1.3

The TCU052EW low frequency, fling time-histories are shown in Figure 4. In this case the acceleration tilt transient occurs at 40.06sec, approximately 8sec earlier than the NS component. The displacement is -352cm (GPS -342cm) the instantaneous tilt acceleration $g\varphi$, is 12.96cm/s/s and φ the instantaneous tilt angle is 13.2mrads. The area of the acceleration tilt profile is 2.98cm/s, the velocity offset. Similarly the area of the velocity step is 180.7cm, which is also the maximum displacement offset as shown in Figure 4, Figure 5 and Figure 6 shows the resulting, corrected time – histories. Moreover, as for the NS component, then on integrating the extracted acceleration transient, it yields the velocity dc shift and displacement offset of the velocity and displacement profile after integrating the acceleration time history. There isn't any other comparable tilt acceleration result published for TCU052.

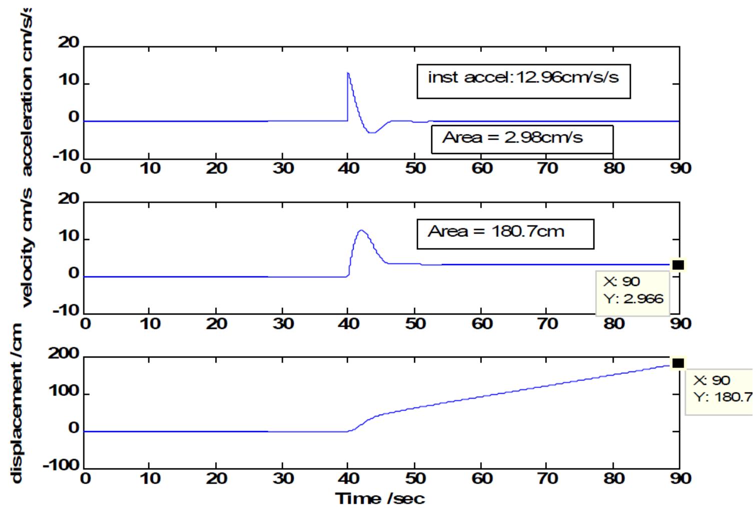

Figure 5. Velocity dc shift and displacement offset after double-integrating the to instantaneous acceleration tilt transient of instrument (A900) to instantaneous acceleration tilt for the TCU052EW component

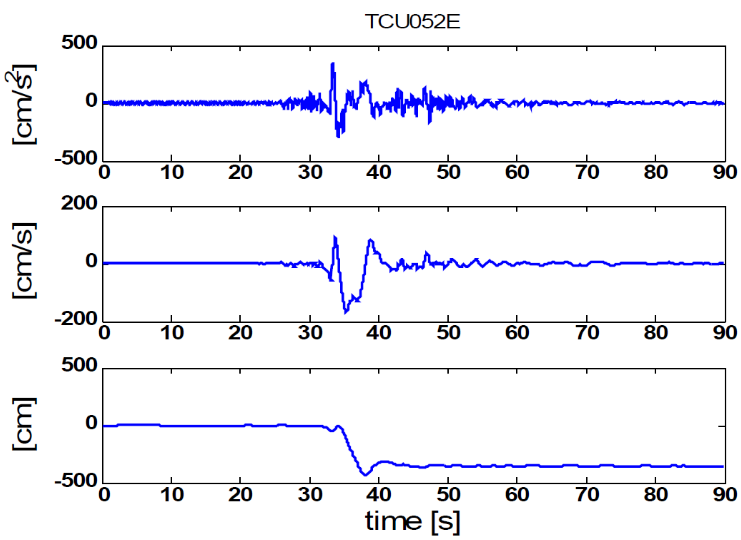

Figure 6. The resultant plots for TCU052EW after the low-frequency sub-bands are added to the higher frequency time histories.

3.2 Results for station TCU129EW

The records from this particular station were referred to in (Boore, 2001) in some detail, when applying a modified correction method due to (Iwan et al, 1985). The wavelet transform produces some interesting acceleration transients (inferred tilt/rotation effects). The time series of Figures 6, 7, 8 show the resulting fling and higher frequency sub-bands for the acceleration, velocity and displacement. Figure 7 shows the low-frequency fling for TCU129EW after the application of the wavelet transform, but before baseline correction. There is clear post-fling distortion in the acceleration. At 30sec there is a δ-pulse like jump (Clinton, 2004) in the acceleration of $g\varphi$ = -4.8 cm/s/s and instantaneous tilt angle φ = 4.9mrads, as that discussed for TCU052. However in addition there is another set of distortions at 40secs up to approx 50sec. This has led to a series of downward steps in velocity giving rise to a velocity shift of -7.5cm/s/s from zero. The profile of these changes in the acceleration, in particular at t > 40sec. Figure 8 shows the effect more clearly, with a spike at 30sec giving a step in velocity, followed by further steps in velocity t >40sec. Of course there isn't any certitude that these distortions are due to tilts/rotations, there are other effects, which could have caused these. However, there is some justification for proposing that these distortions may be due to tilts/rotations.

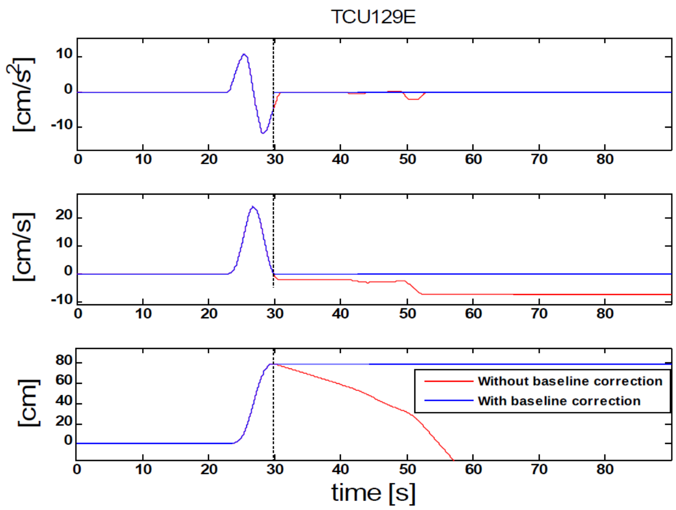

Figure 7. TCU129EW, low-frequency fling before (red) and after (blue) baseline correction, showing tilt/rotation in acceleration and baseline shift in velocity

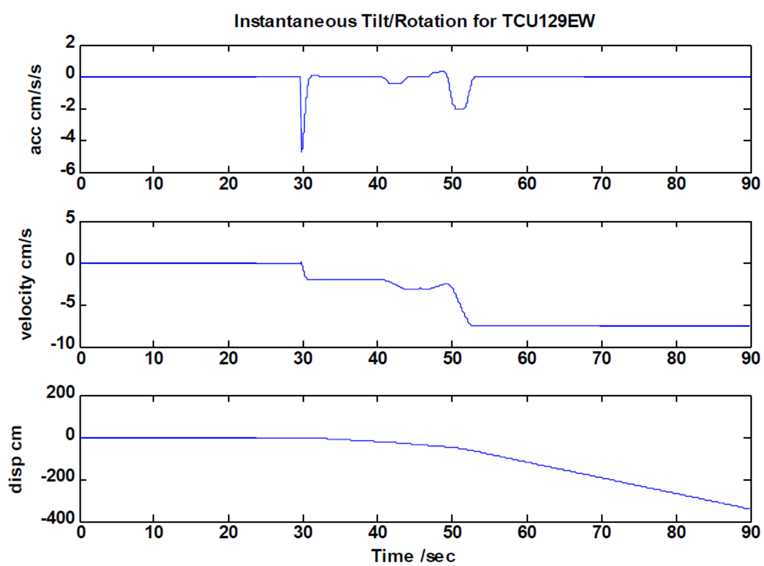

Figure 8. Velocity and displacement response of instrument (A900) to instantaneous acceleration (possible tilt/rotation) transients for the TCU129EW component and their effects after double integration.

The net permanent displacement is shown in Figure 9 as 78.48cm, which is similar to that obtained by (Prof Hung-Chi Chiu, private communication). However his displacement profile shows a peak at 120cm, gradually decaying down to a permanent displacement of just under 80cm after about 70sec, (Boore, 2001), shows a similar profile and peak displacement > 100cm. Whereas the wavelet transform in this case does not show such a peak The GPS station AF11 at 2.3km away shows a permanent displacement of approximately 100cm

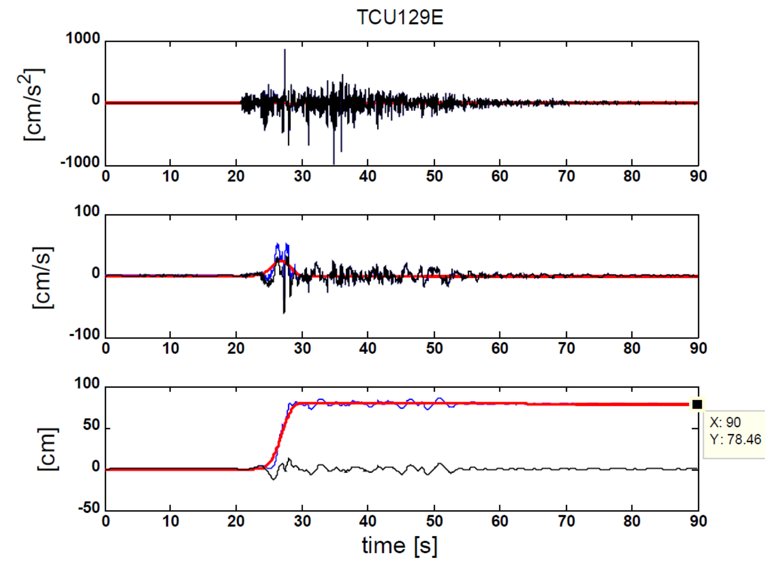

Figure 9. corrected fling (red) and higher frequency sub-bands using bior1.3 for TCU129EW component obtained at level 9, with a displacement of 78.46cm

The time history profiles for TCU129NS are shown in Figure 10 below and in this case the bi-orthogonal 2.6 wavelet was used at level 9 decomposition. At 28.1sec the low-frequency fling showed an acceleration transient of magnitude $g\varphi$ = 9.93cm/s/s, giving a dc shift to the latter part of the velocity time history of 7.65cm/s. The velocity offset after integration then gave a linear trend with a dc offset of 435cm at 90sec. These sorts of baseline errors make double-time integration impossible. However the proposed algorithm then zeroed-out the acceleration from 28.1sec and re-integrated to give the corrected time histories shown below. The GPS displacement for the NS component was -32.1cm, that obtained using the presented wavelet transform method is -26.8cm.

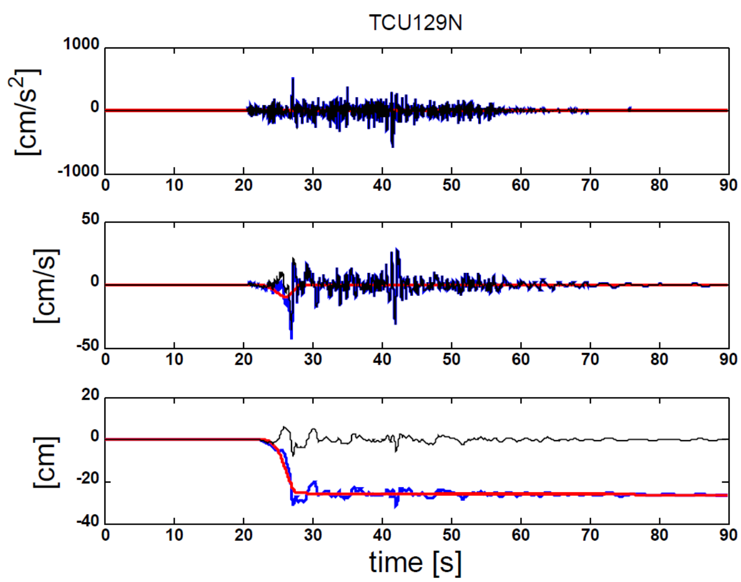

Figure 10. Corrected fling (red) and higher frequency sub-bands using *bior2.6* for TCU129NS component obtained at level 9, with a displacement of -26.8cm. Tilt acceleration transient at 28.1sec, transient magnitude is 9.93cm/s/s

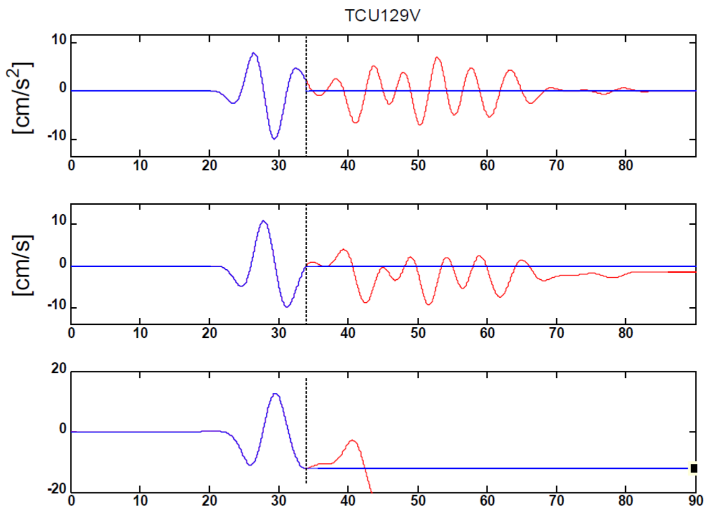

Figure 11. This shows the low-frequency sub-band of the vertical component. The acceleration is very oscillatory, as of course the velocity. However the strong-motion fling is clearly visible, ending at 33.97sec, from which point the oscillatory motion is zeroed out. The first acceleration transient occurs at 33.97sec, with a magnitude of 2.12cm/s/s. The displacement is shown in the figure at -12.26cm, that given by GPS is -17.7cm.

The TCU129V component is interesting because it suggests either at least 9 more tilts, or just a very noisy instrument. In (Boore, 2001) there is a suggestion that the location of the instrument (A900) on a concrete pier may have had an effect on the high- frequency. Certainly there are significant oscillatory effects as can be seen from the time history below. However the fling pulses is clearly visible both in the acceleration and velocity time history and we take the zero velocity cross-over point at 33.97 seconds immediately after the fling pulse in velocity. At that point the acceleration is zeroed to the end of the record and re-integrated, giving a displacement of -12.26cm, the GPS reading for that component is -17.7cm. The acceleration transient, though not explicitly shown is small in magnitude (2.12cm/s/s) compared with that of other components, suggesting its origin may be from instrument noise.

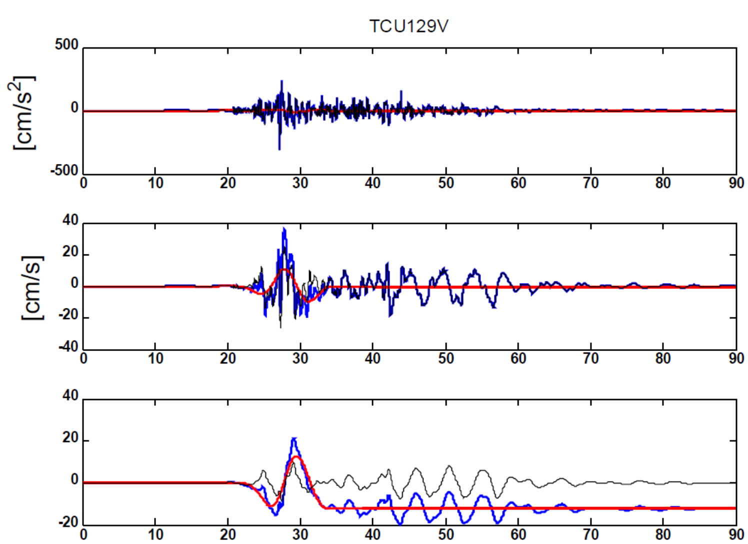

Figure 12. TCU129V corrected vertical component, showing a displacement of -12.26cm compared with -17.7cm GPS. The time histories show the high frequency, low-frequency and resultant time histories by adding the low and high frequency sub-bands.

4. SUMMARY AND CONCLUSION

In conclusion this paper demonstrates the utility of the wavelet transform method (Chanerley, Alexander, 2010) not only to recover the velocity pulse and residual displacement in an automated manner, but in addition the transform also recovers the profile of the baseline error in the form of an acceleration transient embedded in the low-frequency fling and almost sinusoidal time history, moreover it also locates the transient in time. Therefore the application of the transform obviates the need to apply some sophisticated criteria to locate a suitable time point(s). Moreover it can be inferred that for some of the components the acceleration transients may be due to tilts/ground rotations, whereas other components and in particular those in the vertical direction may be due to noise. The vertical component is less sensitive to tilts/rotations (Graizer 2005), therefore it is likely their acceleration transients are due to instrument or other noise. The summary of results is as follows:

Table 1. Results for TCU129 and TCU052

Chi-Chi Station	N-S Components		E-W Components		Vertical Components	
	Tilt Acc	Time	Tilt Acc	Time	Tilt Acc	Time
	cm/s/s	sec	cm/s/s	sec	cm/s/s	sec
TCU129	9.93	28.1	-4.8	30	2.12	33.97
TCU052	3.015	48.45	12.96	40.06	3.15	44.23

Table 2. Estimates of permanent displacement for TCU052

Level	TCU052NS	TCU052EW	TCU052V
	[cm]	[cm]	[cm]
10	671	-352	369
GPS	845.1	-342.3	397

Table 3. Estimates for permanent displacement for TCU129

Level	TCU129NS	TCU129EW	TCU129V
	[cm]	[cm]	[cm]
9	78.46	-26.8	-12.26
GPS	88.2	-32.1	-17.7

In themselves the results are inconclusive in the sense that the two stations are isolated because the distances between the two stations station are considerable. However there is some consistency in the occurrence of the acceleration transients in TCU129, but less consistency for TCU052. The displacements show reasonable correlation with GPS readings.

In conclusion it can be seen that the wavelet transform method proposed by (Chanerley and Alexander, 2010) is a reasonable method for obtaining displacements. In addition the method can isolate the low-frequency fling profile and estimate 'spike' like acceleration transients, which prevent double-time integration, but which the algorithm easily removes. These can be inferred as due to tilts/rotations, though in the case of the vertical component are more likely due to noise.

REFERENCES

Akkar S, Boore D M, (2009) 'On baseline correction and uncertainty in response spectra for baseline variations commonly encountered in digital accelerographs', *Bull Seismol Soc Am.,* 99: 9, 1671-90

Berrill, J, et al (2011), 'The Canterbury Accelerograph Network (CanNet) and some Results from the September 2010, M7.1 Darfield Earthquake', *Proc of the 9th Conf on Earthquake Eng.*, 14-16th April 2011, Auckland, New Zealand

Boore D M., (2001), ‘Effect of Baseline Corrections on Displacements and Response Spectra for Several Recordings of the 1999 Chi-Chi, Taiwan Earthquake’, *Bull Seismol Soc Am.,* 91, 1199-1211

Chanerley A A**,** Alexander N A, (2010) 'Obtaining estimates of the low-frequency ‘fling’, instrument tilts and displacement timeseries using wavelet decomposition', *Bulletin of European Earthquake Engineering*, 8:231-255 http://dx.doi.org/10.1007/s10518-009-9150-5

Chanerley, A A, Alexander N A, Halldorsson B, Sigbjornsson R, Perryman R, (2010) ‘Baseline Correction made easy using an Automated Method based on the Wavelet Transform’, *Proc of the 9th US National and 10th Canadian Conference on Earthquake Engineering*, paper 358, July 25th-29th,Toronto, Canada

Chanerley A. A., Alexander N.A. (2007) “Correcting Data from an unknown Accelerometer using Recursive Least Squares and Wavelet De-noising”, *Journal of Computers and Structures* (85) 21-22, pp 1679-1692

Chanerley A A**,** Alexander N A, Halldorsson B, (2009). 'On fling and baseline correction using quadrature mirror filters', *12th International Conference on Civil, Structural and Environmental Engineering Computing*, paper 177, Madeira, Portugal,1-4 September " doi:10.4203/ccp.91.177

Chanerley A. A., Alexander, N A. (2008) “Using the Total Least Squares method for Seismic Correction of recordings from unknown instruments”, (2008) (39), pp849-860, *Journal of Advances in Engineering Software.*

Chanerley, A A, ISSEE, *Intl Symposium on Strong Motion Earthquake Effects*, May 2009: www.eerc.hi.is

Chen, S-M, Loh C-H, (2006) “Estimates of Permanent Ground Displacements from Near-fault, Strong-Motion Accelerograms”, *1st European Conference of Earthquake Engineering & Seismology”*, paper 1631, Geneva, 3-8 Sept

Chiu, H-C, (1997), ‘Stable baseline correction of Digital Strong Motion Data’, *Bull Seismol Soc Am* 87, 932-944

Coifman R., Donoho D L, (1995), ‘Translation Invariant De-noising, Wavelets and Statistics’, *Lecture Notes in Statistics*, Vol 103, Springer, New York, pp 125-150

Coifman R R, Wickerhauser M V, (1993) ‘Wavelets and Adapted Waveform Analysis’, *Proc Symposia in Appl Mathematics*, Volume 47, American Mathematics Soc., pp 119-153, Providence, Rhode Island.

Debauchies I., (1992), ‘Ten Lectures on Wavelets’, SIAM, Philadelphia

Grazier V.,(1979), ‘Determination of the True Ground Displacements by using Strong Motion Records’, *Izvestiya Phys Solid Earth*, 15, 875-885

Grazier V.,(2005), ‘Effects of Tilt on Strong Motion Data Processing’, *Soil Dyn Earthq Eng* 25:197-204

Iwan WD., Moser MA., Peng CY., (1985) ‘Some Observations on Strong-Motion Earthquake Measurements using a Digital Accelerograph’, *Bull Seismol Soc Am* 99, 1225-1246

Mallat S, (1989) ‘A Theory for Multiresolution Signal Decomposition: The Wavelet Representation’, *IEEE Pattern Analysis and Machine Intelligence*, 11:7 pp674-693